

Three-dimensional atomic-scale mapping of Pd in $\text{Ni}_{1-x}\text{Pd}_x\text{Si}/\text{Si}(100)$ thin films

Yeong-Cheol Kim

Dept. of Materials Engineering, Korea University of Technology and Education, Cheonan, Chungnam 330-708, Korea

Praneet Adusumilli, Lincoln J. Lauhon,^{a)} and David N. Seidman

Department of Materials Science and Engineering, Northwestern University, Evanston, Illinois 60208-3108, USA

Soon-Yen Jung and Hi-Deok Lee

Dept. of Electronics Engineering, Chungnam National University, Daejeon 305-764, Korea

Roger L. Alvis, Rob M. Ulfing, and Jesse D. Olson

Imago Scientific Instruments Corporation, 5500 Nobel Drive, Madison, Wisconsin 53711, USA

(Received 25 July 2007; accepted 22 August 2007; published online 12 September 2007)

Atom-probe tomography was utilized to map the three-dimensional distribution of Pd atoms in nickel monosilicide thin films on Si(100). A solid-solution $\text{Ni}_{0.95}\text{Pd}_{0.05}$ film on a Si(100) substrate was subjected to rapid thermal processing plus steady-state annealing to simulate the thermal processing experienced by NiSi source and drain contacts in standard complementary metal-oxide-semiconductor processes. Pd is found to segregate at the $(\text{Ni}_{0.95}\text{Pd}_{0.05})\text{Si}/\text{Si}(100)$ heterophase interface, which may provide a previously unrecognized contribution to monosilicide stabilization. The silicide-Si heterophase interface was reconstructed in three dimensions on an atomic scale and its chemical roughness was evaluated. © 2007 American Institute of Physics. [DOI: 10.1063/1.2784196]

NiSi is an important material for contact applications in the semiconductor industry as it transitions from the 65 nm technology node to the 45 nm node.¹ The Ni–Si reaction has been extensively studied since the 1970s.^{2–14} Recent efforts are focusing on the formation of the NiSi phase and its relative stability.^{15–18} The major advantages of NiSi over TiSi_2 and CoSi_2 contacts include a lower temperature of formation, lower resistivity in narrow dimensions, reduced Si consumption, and formation kinetics that are controlled by diffusion of Ni, which leads to significantly smoother heterophase interfaces. Additionally, a one step annealing can be used for the self-aligned silicide process.¹⁹ The main drawbacks of this system include (a) agglomeration of the desired NiSi phase, which causes an increase in the resistivity, and (b) formation of the higher resistivity NiSi_2 phase at elevated processing temperatures. Recent studies demonstrate that adding elements such as Pd, Pt, or Rh reduces the agglomeration of thin NiSi films and increases the formation temperature of NiSi_2 .²⁰ Herein, we report on the use of laser-assisted local-electrode atom-probe (LEAP®) tomography to map the atomic-scale distribution of Pd in annealed $\text{Ni}_{(1-x)}\text{Pd}_x/\text{Si}(100)$ films. Under typical thermal processing conditions, a fraction of the Pd segregates at the NiSi/Si(100) heterophase interface, while the root-mean-squared chemical roughness of the interface remains less than 1 nm.

$\text{Ni}_{(1-x)}\text{Pd}_x$ ($x=0.01, 0.05, 0.10$) films were deposited by rf magnetron sputtering on *p*-type Si(100) substrates after removing the native oxide using a 2% buffered HF solution. The films were subjected to rapid thermal processing (RTP) for 30 s at different temperatures, after which the unreacted

NiPd alloy was selectively removed with $\text{H}_2\text{SO}_4 + \text{H}_2\text{O}_2$. Using sheet resistance measurements as an indicator of the formation and persistence of the monosilicide phase, it was determined that $\text{Ni}_{0.95}\text{Pd}_{0.05}$ has the broadest thermal processing window of the three compositions studied (Fig. 1). On this basis, the $\text{Ni}_{0.95}\text{Pd}_{0.05}/\text{Si}$ sample that underwent RTP at 600 °C was selected for further study; all measurements discussed are for this sample. This sample was next annealed at 650 °C for 30 min in an N_2 ambient to approximate the effects of subsequent thermal treatments experienced by silicide contacts in the remainder of the complementary metal-oxide-semiconductor fabrication process. Scanning electron microscopy imaging (not shown) revealed that the annealing treatment increased the thickness of the silicide layer and x-ray diffraction confirmed that nickel monosilicide (NiSi) was the only silicide phase present (not shown). No diffraction peaks corresponding to NiSi_2 or PdSi were detected.

To explore the role of Pd in stabilizing the NiSi phase, an Imago Scientific Instruments LEAP® tomograph was

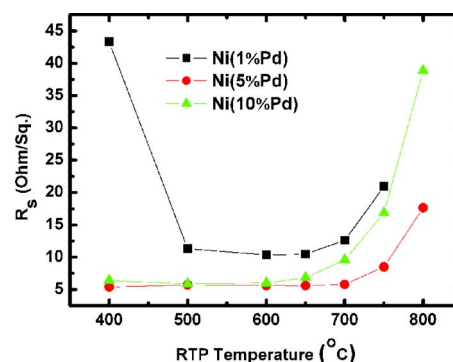


FIG. 1. (Color online) Sheet resistance measurements for $(\text{Ni}_{1-x}\text{Pd}_x)\text{Si}/\text{Si}(100)$ thin films following rapid thermal processing for 30 s.

^{a)}Electronic mail: lauhon@northwestern.edu

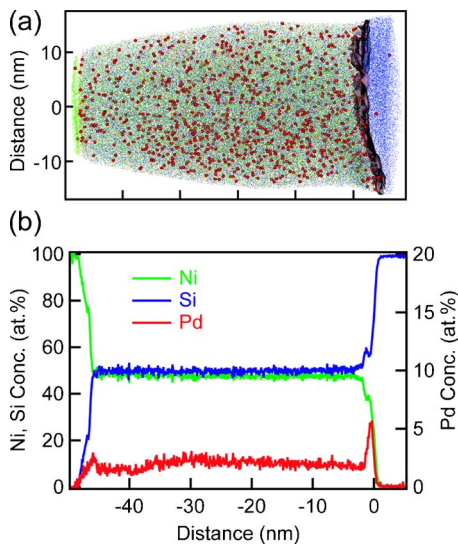


FIG. 2. (Color online) (a) Two-dimensional projection of the full three-dimensional reconstruction of local-electrode atom-probe (LEAP®) tomography data showing the distribution of elements (colored points) and the isoconcentration surface (shaded sheet) that defines the heterophase interface. Ni, Si, and Pd atoms are shown in green, blue, and red, respectively. Pd atoms are enlarged and only 10% of the Si atoms are shown for clarity. Within the NiSi phase, the Pd is seen to be distributed uniformly. The Ni atoms at top are from a protective capping layer. (b) Proxigram (proximity histogram) displaying the concentrations of Ni, Si, and Pd vs film depth. Concentrations were calculated for a series of isoconcentration surfaces moving into the thin film; the NiSi/Si heterophase interface provides an example of an isoconcentration surface.

used to analyze the chemical concentration of each element with subnanoscale spatial resolution in three dimensions.²¹ LEAP® tomographic samples were prepared using a dual-beam focused ion-beam (FIB) microscope and the so-called “lift-out” technique.^{22,23} The tips were ion milled to achieve an end radius of approximately 50 nm. A pulsed picosecond laser operating at 250 kHz with an energy per pulse of 0.5 nJ was used to dissect the specimen on an atom-by-atom basis, which was held at 40 K under ultrahigh vacuum conditions ($<10^{-10}$ Torr).^{24,25}

Figure 2 displays the LEAP® tomographic results in two representations. Figure 2(a) presents a two-dimensional projection of the full three-dimensional reconstruction for an analysis volume of $30 \times 30 \times 60$ nm³. Figure 2(b) presents a proximity histogram (or proxigram), which is a three-dimensional nonlinear composition profile created by calculating the average composition of a series of isoconcentration surfaces as these surfaces are advanced into the film.²⁶ Both figures demonstrate that the distribution of Pd is uniform within the silicide film. We therefore conclude that the thermal processing was sufficient to achieve the equilibrium distribution of Pd. Furthermore, the sum of the Pd and Ni concentrations is 50 at. %, suggesting that the Pd atoms are sitting substitutionally on the Ni sublattice of NiSi. This is in agreement with the fact that Pd and Ni monosilicides are known to be mutually soluble.²⁰ Interestingly, the proxigram in Fig. 2(b) also reveals the segregation of Pd atoms at the NiSi/Si heterophase interface as indicated by the narrow Pd peak at this interface. The thermodynamic driving force for Pd segregation is the decrease in the interfacial Gibbs free energy associated with the Ni_(1-x)Pd_x/Si(100) heterophase interface. The segregation of a solute species at a heterophase interface is quantified by the Gibbsian interfacial

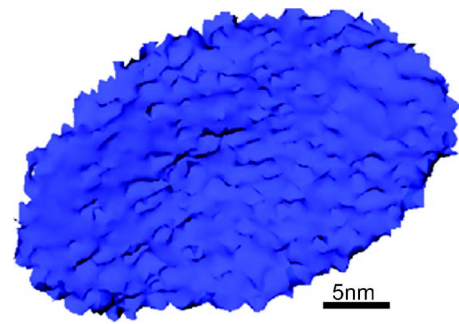


FIG. 3. (Color online) Two-dimensional projection of the three-dimensional reconstruction of the silicide-Si interface based on a Si isoconcentration surface. The root-mean-squared chemical roughness of this interface is 0.8 nm.

excess of solute Γ_s which is given by $\Gamma_s = (\sum C_n - C_0/A_n)/(1 - C_0)$ and $A_1 = N_1/\rho\Delta l$, where A_1 is the effective area of a slice at proximity l , N_1 is the number of atoms in the slice, Δl is the shell thickness, and ρ is the ideal atomic density of Ni_{0.95}Pd_{0.05}Si. The proxigram of Fig. 2(b) yields a discrete count of the atoms in the vicinity of this heterophase interface, thus permitting a direct measurement of Γ_s .²⁷ The Gibbsian interfacial excess of Pd at the heterophase interface is determined to be 3.4 ± 0.2 atom/nm². This interfacial Pd, which has not been observed previously, may play a role in stabilizing the nickel monosilicide phase, as discussed further below.

The addition of small amounts of Pd to Ni films on Si(100) is known to have two beneficial effects on the nickel monosilicide phase formed with RTP.²⁰ First, the agglomeration of thin [Ni_(1-x)Pd_x]/Si films under further thermal processing is diminished compared to pure NiSi. Second, the nucleation and growth of NiSi₂ are pushed to higher temperatures. The agglomeration of thin, uniform pure NiSi films on Si(100) is driven by a decrease in the interfacial Gibbs free energy that is achieved by reducing the contact area between the two phases. The enhanced resistance of (Ni_{1-x}Pd_x)/Si to agglomeration has been attributed to the reduction in the silicide-Si interfacial free energy by diffusion of Pd to that interface.²⁰ The observation of excess interfacial Pd provides the first direct evidence in support of this argument, though it is important to note that additional research must be performed to determine whether Pd segregation is a necessary or sufficient condition for morphological stabilization. Multiple arguments have been put forward to explain why Pd inhibits the formation of the disilicide phase, but the arguments involve changes in the free energies of bulk, not interfacial phases.^{20,28} The results presented herein suggest that an interfacial phase may also contribute to bulk phase stabilization.

LEAP® tomography provides additional information not present in more conventional analyses, including the ability to visualize chemical inhomogeneities at a buried interface (Fig. 3). The three-dimensional real space view of the (Ni_{0.98}Pd_{0.02})/Si/Si interface displayed in Fig. 3 is a silicon isoconcentration surface with a root-mean-squared chemical roughness of approximately 0.8 nm. Quantitative measurements of interfacial inhomogeneities can be usefully correlated with important electronic properties including resistivity, barrier height, and local work function.²⁹ This direct nanoscale measurement represents an improvement over other methods, such as light scattering, in which the smooth-

ness of the silicide/silicon interface is averaged over much larger sample regions.³⁰

In summary, we have mapped the three-dimensional nanoscale distribution of Pd in the monosilicide and at the nickel silicide-silicon interface. We find that the Pd distribution is uniform within the $(\text{Ni}_{0.98}\text{Pd}_{0.02})\text{Si}$ phase but greatly enhanced at the $(\text{Ni}_{0.98}\text{Pd}_{0.02})\text{Si}/\text{Si}$ heterophase interface over a length scale of 1 nm. Interfacial Pd may therefore play a role in stabilizing NiSi against agglomeration and transformation to NiSi_2 .

This research is supported by Semiconductor Research Corporation, Task No. 1441.001. Professor Yeong-Cheol Kim is an Imago Scientific Instruments Senior Fellow (2006–2007) and acknowledges their partial support. One of the authors (L.J.L.) acknowledges support of an Alfred P. Sloan Foundation fellowship. Professor Y. Rosenwaks is thanked for discussions and Research Professor D. Isheim is thanked for managing the Northwestern Center for Atom-Probe Tomography (NUCAPT).

¹Front End Processes, International Technology Roadmap for Semiconductors, 2005.

²K. E. Sundstrom, S. Petersson, and P. A. Tove, *Phys. Status Solidi A* **20**, 653 (1973).

³N. F. Podgrushko, N. F. Selivanova, and L. A. Dvorina, *Izv. Akad. Nauk SSSR, Neorg. Mater.* **10**, 150 (1974).

⁴S. Petersson, E. Mgbenu, and P. A. Tove, *Phys. Status Solidi A* **36**, 217 (1976).

⁵K. Nakamura, J. O. Olowolafe, S. S. Lau, M. A. Nicolet, J. W. Mayer, and R. Shima, *J. Appl. Phys.* **47**, 1278 (1976).

⁶R. Pretorius, C. L. Ramiller, S. S. Lau, and M. A. Nicolet, *Appl. Phys. Lett.* **30**, 501 (1977).

⁷K. N. Tu, *J. Appl. Phys.* **48**, 3379 (1977).

⁸T. G. Finstad, J. W. Mayer, and M. A. Nicolet, *Thin Solid Films* **51**, 391 (1978).

⁹R. Anderson, J. Baglin, J. Dempsey, W. Hammer, F. d'Heurle, and S. Petersson, *Appl. Phys. Lett.* **35**, 285 (1979).

¹⁰J. E. E. Baglin, H. A. Atwater, D. Gupta, and F. M. d'Heurle, *Thin Solid Films* **93**, 255 (1981).

¹¹T. G. Finstad, *Phys. Status Solidi A* **63**, 223 (1981).

¹²G. Ottaviani, K. N. Tu, and J. W. Mayer, *Phys. Rev. B* **24**, 3354 (1981).

¹³N. W. Cheung, P. J. Grunthaner, F. J. Grunthaner, J. W. Mayer, and B. M. Ullrich, *J. Vac. Sci. Technol.* **18**, 917 (1980).

¹⁴F. d'Heurle, C. S. Petersson, J. E. E. Baglin, S. J. La Placa, and C. Y. Wong, *J. Appl. Phys.* **55**, 4208 (1984).

¹⁵C. Lavoie, R. Purtell, C. Cöia, C. Detavernier, P. Desjardins, J. Jordan-Sweet, C. Cabral, F. M. d'Heurle, and J. M. E. Harper, *Proc.-Electrochem. Soc.* **11**, 455 (2002).

¹⁶F. M. d'Heurle, *J. Electron. Mater.* **27**, 1138 (1998).

¹⁷S. L. Zhang, *Microelectron. Eng.* **70**, 174 (2003).

¹⁸C. Lavoie, C. Detavernier, and P. Besser, in *Nickel Silicide Technology*, edited by L. J. Chen, C. Lavoie, C. Detavernier, and P. Besser (IEE, London, 2004), Vol. 5, pp. 95–151.

¹⁹T. Morimoto, T. Ohguro, H. S. Momose, T. Iinuma, I. Kunishima, K. Suguro, I. Katakabe, H. Nakajima, M. Tshuchiaki, M. Ono, Y. Katsumata, and H. Iwai, *IEEE Trans. Electron Devices* **42**, 915 (1995).

²⁰C. Lavoie, C. Detavernier, C. Cabral, Jr., F. M. d'Heurle, A. J. Kellock, J. Jordan-Sweet, and J. M. E. Harper, *Microelectron. Eng.* **83**, 2042 (2006).

²¹D. N. Seidman, *Annu. Rev. Mater. Res.* **37**, 127 (2007).

²²K. Thompson, D. Lawrence, D. J. Larson, J. D. Olson, T. F. Kelly, and B. Gorman, *Ultramicroscopy* **107**, 131 (2007).

²³The “lift-out” process was performed using an FEI Nova dual beam FIB and Omniprobe sample manipulator. An FEI DB620 was used for coarse and fine sharpening. Prior to ion milling, 75 nm of Ni and 100 nm of Pt were deposited by sputtering and ion beam deposition, respectively. A 30 kV Ga ion beam was used for coarse ion milling to produce a tip diameter of less than 300 nm; the Ga ion penetration depth is 30 nm in Si, and less than that in Pt, preventing ion damage in the silicide region of interest. A 5 kV (5 nm penetration depth) beam was used for fine sharpening, removing most of the Pt cap but leaving the Ni cap in place. The atom probe measurement itself was used to verify that Ga implantation induced intermixing did not occur during sharpening.

²⁴D. E. Perea, J. L. Lensch, S. J. May, B. W. Wessels, and L. J. Lauhon, *Appl. Phys. A: Mater. Sci. Process.* **85**, 271 (2006).

²⁵T. F. Kelly and M. K. Miller, *Rev. Sci. Instrum.* **78**, 031101 (2007).

²⁶O. C. Hellman, J. A. Vandenbroucke, J. Rüsing, D. Isheim, and D. N. Seidman, *Microsc. Microanal.* **6**, 437 (2000).

²⁷A detailed description of the calculation of Gibbsian interfacial excess using atom-probe tomography data appears in O. C. Hellman and D. N. Seidman, *Mater. Sci. Eng., A* **327**, 24 (2002).

²⁸J. F. Liu, J. Y. Feng, and J. Zhu, *Appl. Phys. Lett.* **80**, 270 (2002).

²⁹Th. Gatzel, S. Sadewasser, R. Shikler, Y. Rosenwaks, and M. Ch. Lux-Steiner, *Mater. Sci. Eng., B* **102**, 138 (2003).

³⁰S. R. Naik, S. Rai, G. S. Lodha, and R. Brajpuriya, *J. Appl. Phys.* **100**, 013514 (2006).